



*Bogoliubov Laboratory of Theoretical Physics
Joint Institute for Nuclear Research*



SMALL ATOMIC He CLUSTER AT LOW ENERGIES

Elena Kolganova (BLTP JINR)

*September 30 – October 4, 2024,
Khabarovsk, Russia*

Outline

- Few –Body Systems:
 - What is known about Helium
 - Dimer, Trimer - Experiments
 - *Efimov effect*
 - Formalism: Faddeev differential equations – *A.Korobitsin talk*
- Some Results:
 - $^4\text{He}_3$ and $^3\text{He}-^4\text{He}_2$ - Helium Trimers – *A.Korobitsin talk*
- Conclusion

Helium

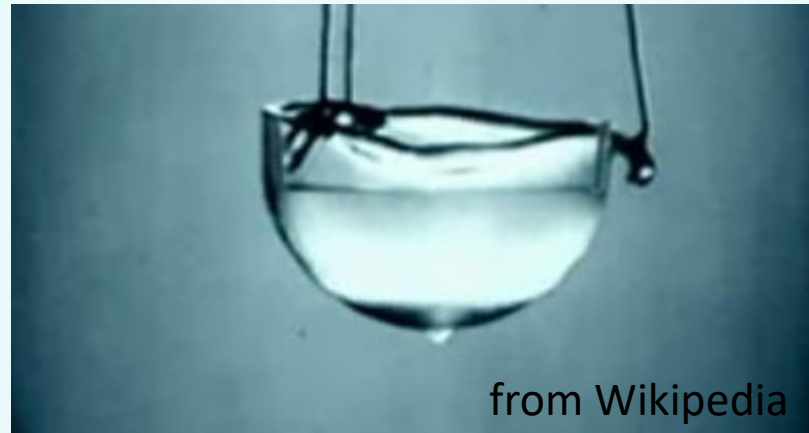
- The first evidence for the existence of helium was a new spectral feature in the Fraunhofer spectrum of the sun discovered in 1868 by the French astronomer Jules Jansen.
- Helium is the second most abundant element in the universe after hydrogen.
- Helium was first liquified by Hejke Kamerlingh-Onnes in 1908 cooling it at 4.17 K.
- In 1938, the superfluidity of liquid helium was discovered at temperatures below 2.14 K by Pyotr Kapitza.

Superfluid Bulk Helium-4

- ^4He is the only substance that remains liquid under normal pressure at
- zero temperature (superfluid with condensate fraction of around 8%).
- normal to superfluid transition at 2.17K.

Bulk liquid helium-4:
Binding energy per
particle $E/N \approx -7\text{K}$

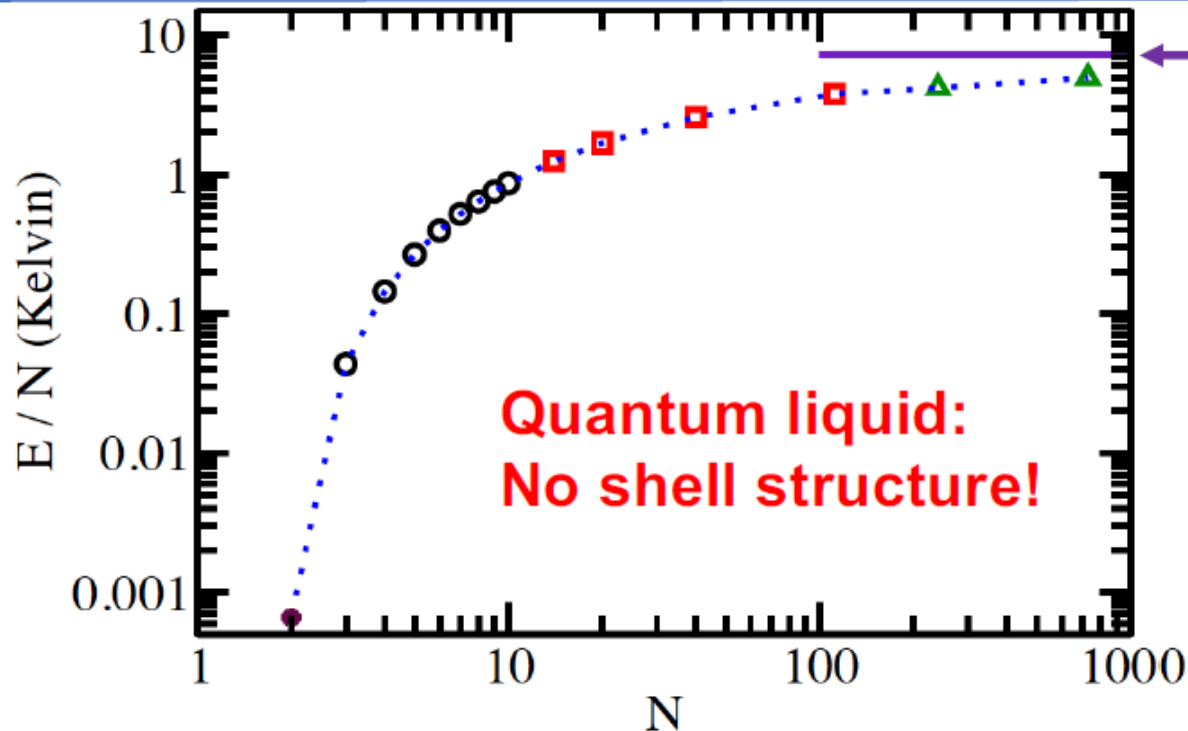
(1 K = 8.6×10^{-5} eV).



from Wikipedia

Liquefied helium. The drop of liquid at the bottom of the glass represents helium spontaneously escaping from the container over the side, to empty out of the container.

Helium Droplets = Quantum Liquid



Well known literature results:

Small N ($N < 10$):
 $E/N \sim \# N$.

(E/N changes by four orders of magnitude.)

$N > 20$ energies are well described by liquid drop model with volume and surface terms (no Coulomb, asymmetry, or pairing terms).

Rich interplay between many-body nuclear physics and quantum droplet community [e.g., Pandharipande et al., PRL 50, 1676 (1983); Stringari et al., JCP 87, 5021 (1987); Sindzingre et al., PRL 63, 1601 (1989)].

Helium

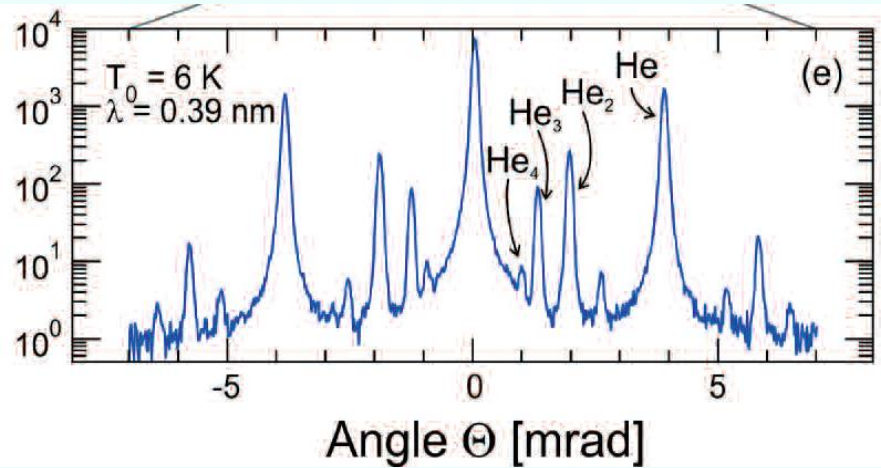
- The helium atom is **the most inert of all atoms**. No chemistry is known. In comparison with the simpler H atom, the He atom, with two electrons in a closed shell, is even **smaller in size** and has a three times smaller polarizability.
- The inertness of the helium atom is responsible for the **an extremely weak van der Waals interaction** between two helium atoms, which was a reason for a long standing debates about existence of the helium dimer, until it was experimentally observed in 1990s.

Molecules in Superfluid Helium Nanodroplets

Spectroscopy, Structure, and Dynamics

Ed.: A.Slenczka & J.P. Toennies (Springer,2022) **Topics in Applied Physics, V. 145**

Matter wave diffraction experiment



Louis de Broglie wavelength

$$\lambda = \frac{h}{M v}$$

The Diffraction angle

$$\sin \theta = n \frac{\lambda}{d} = n \frac{h}{d N m v}$$

m — mass of helium atom

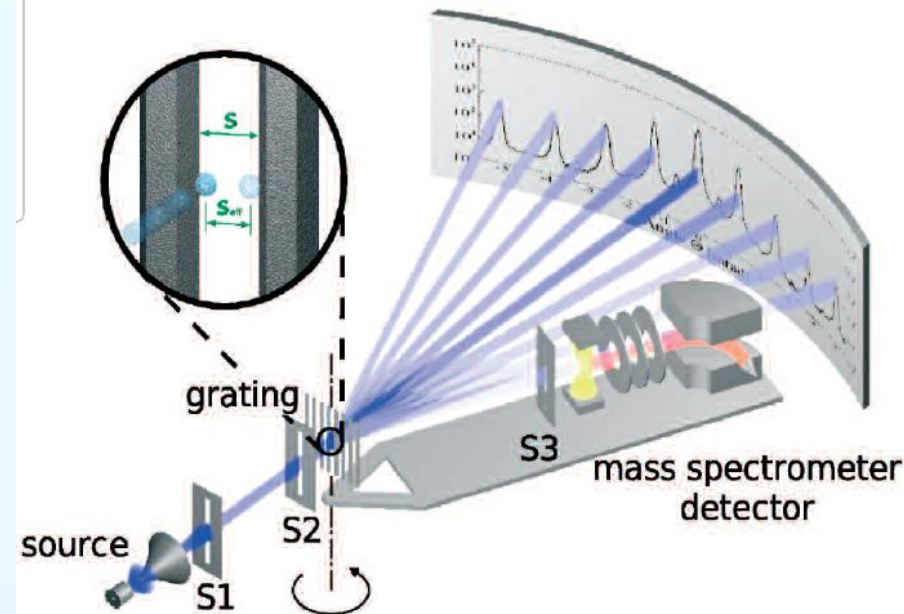
N — number of helium atoms

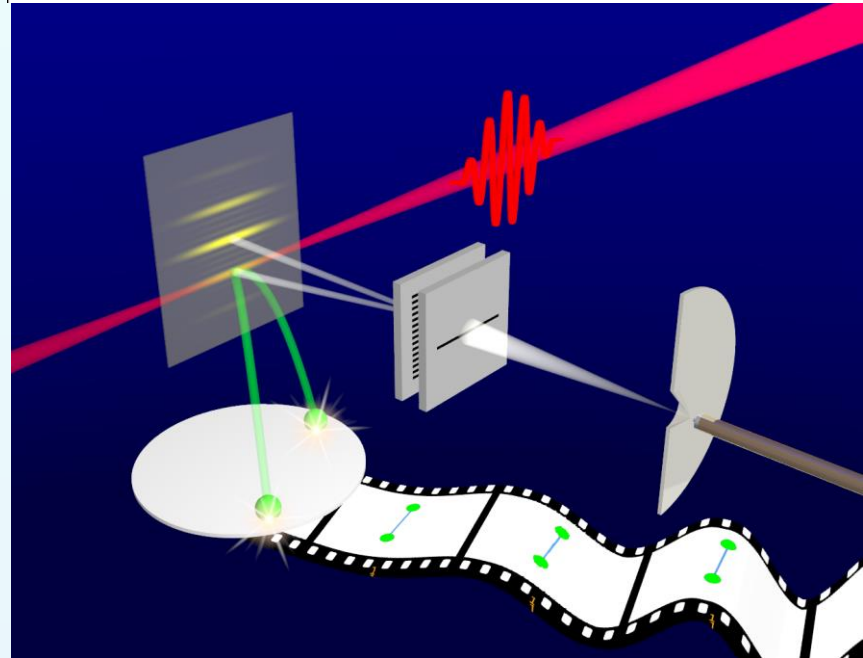
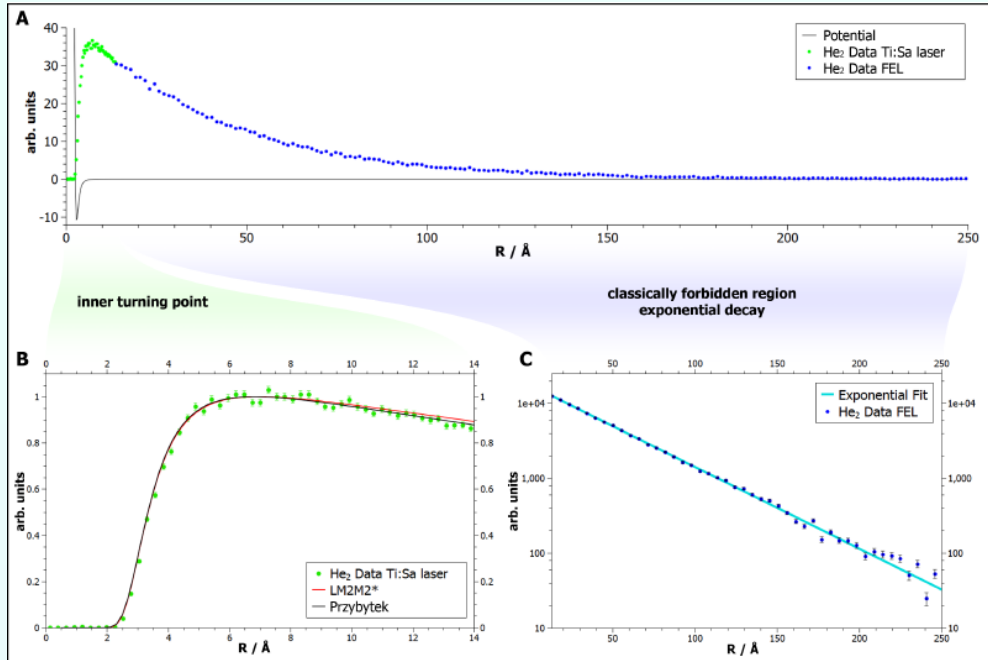
$M = N m$ — mass of cluster

v — velocity

n — diffraction order

Schematic diagram of the cluster beam apparatus used for the diffraction of small He clusters in nozzle beam expansion exps.





Experimental measurement of the helium dimer wavefunction (A).

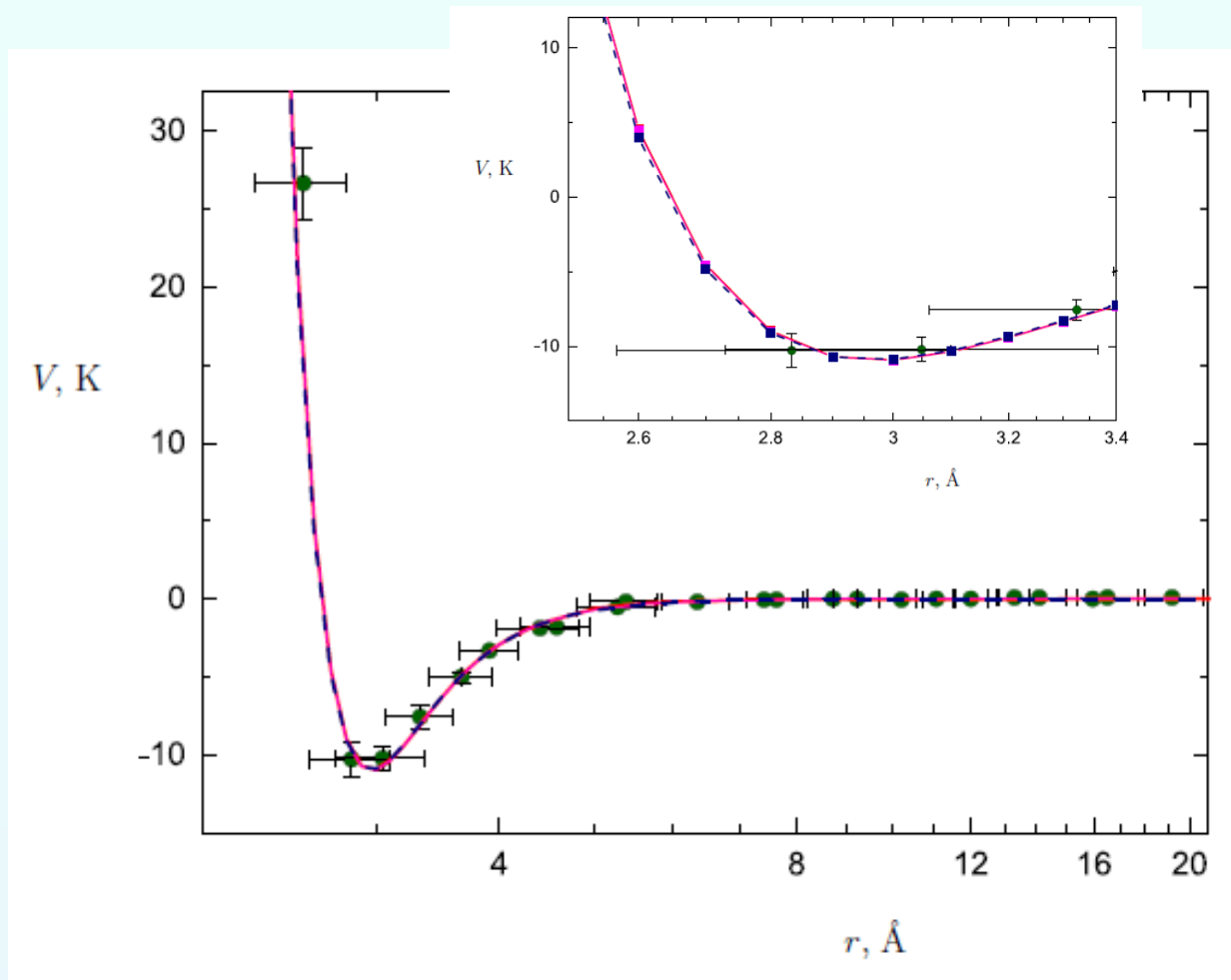
Two detailed views show the important features of this quantum system: The region of the inner turning point (B) is in agreement with theoretical predictions with LM2M2 and Przybytek potentials, and the exponential decay in the classical forbidden region (C).

A helium dimer binding energy of **151.9 ± 13.3 neV ($1.76_{-0.15}^{+0.15}$ mK)** is obtained from the exponential slope.

$$\langle R \rangle = 52 \pm 4 \text{ \AA}$$

FLASH's X-rays (red) ionize both helium atoms of the molecule, causing them to separate in an explosive manner. The ions are then imaged on a location-resolving detector, symbolised by the film strip. The wave function is then reconstructed from a multitude of individual images.

INTERACTION POTENTIALS



He-He potential $V(r)$, points are experimental data from **S. Zeller et al.**
Phys. Rev. Lett 121 (2018) 083002, blue curve – HFD-B potential (by R.A.Aziz et al.),
red curve – PRZ2010 (by M. Przybytek et al.).

INTERACTION POTENTIALS

Potential models:

– Lennard - Jones [1]: $V(r) = 4 \varepsilon \left[\left(\frac{\sigma}{r} \right)^{12} - \left(\frac{\sigma}{r} \right)^6 \right]$
 ε – scales the energy and σ – the length scale;

– Tang -Toennies [2]:

where A and b parameters,

the C_{2n} are the dispersion coefficient,

$f_{2n}(bR)$ - the damping function,

which is given by the following expression:

$$f_{2n}(x) = 1 - e^{-x} \sum_{k=0}^{2n} \frac{x^{-k}}{k!}$$

– Aziz [3]: $V(x) = \varepsilon V_b(\zeta)$

where $\zeta = x/r_m$, and term $V_b(\zeta)$ has the form:

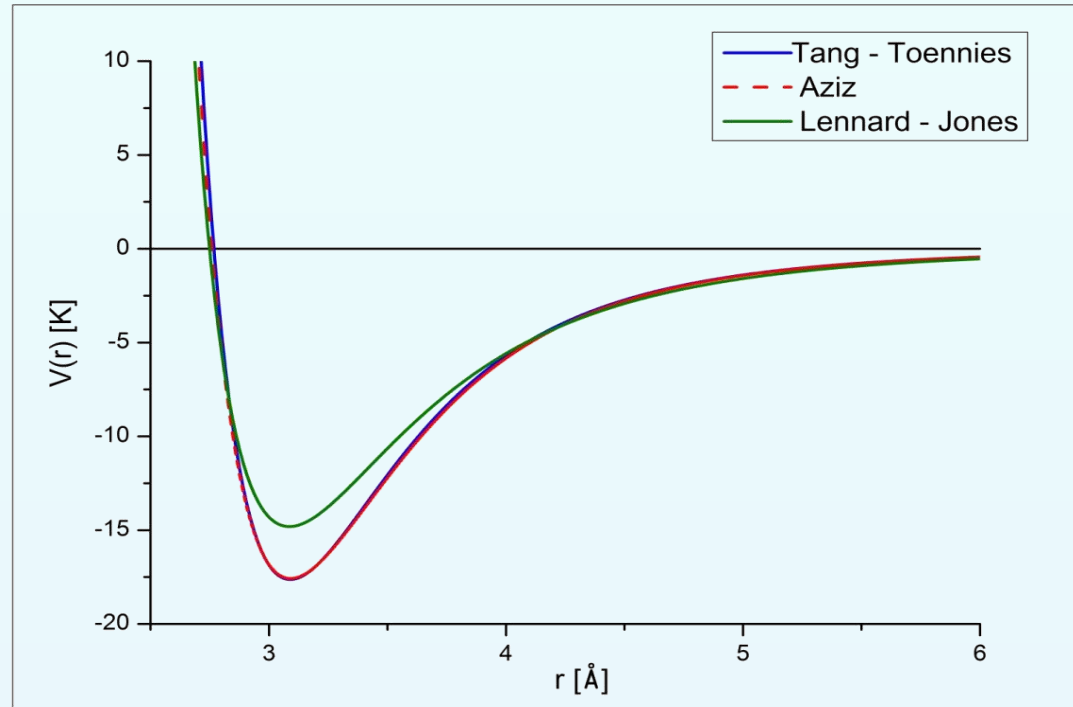
$$V_b(\zeta) = A \exp(-\alpha \zeta + \beta \zeta^2) - \left[\frac{C_6}{\zeta^6} + \frac{C_8}{\zeta^8} + \frac{C_{10}}{\zeta^{10}} \right] F(\zeta)$$

at that x is expressed in the same length units as r_m (for this case they are angstroms).

Function $F(\zeta)$ is given by the expression:

$$F(\zeta) = \begin{cases} \exp[-(D/\zeta - 1)^2], & \text{if } \zeta \leq D, \\ 1, & \text{if } \zeta > D. \end{cases}$$

$$V(R) = V_{rep} + V_{att} = A e^{-bR} - \sum_{n=3}^N f_{2n}(bR) \frac{C_{2n}}{R^{2n}}$$



[1] D.M. Leither, J.D. Doll, R.M.Whitnell // J.Chem.Phys. **94**, 6644 - 6659 (1991)

[2] K.T. Tang and J.P. Toennies // J.Chem.Phys. **118**, 4976 - 4983,(2003)

[3] R.A. Aziz and M.J. Slaman // J. Chem. Phys. **94**, 8047 - 8053 (1991);

D.A. Barrow, M.J. Slaman, R.A. Aziz // J. Chem. Phys. **91**, 6348-6358 (1989);

R.A. Aziz // J. Chem. Phys. **99**, 4518 - 4525 (1993)

Potential models: PRZ2010 [6] and PRZ2017 [7]

$$V(R) = V_{BO}(R) + V_{ad}(R) + V_{rel}(R) + V_{QED}(R)$$

$V_{BO}(R)$ - nonrelativistic Born - Oppenheimer (BO),

$V_{ad}(R)$ - adiabatic correction,

$V_{rel}(R)$ - relativistic correction,

$V_{QED}(R)$ - quantum electrodynamics (QED).

R	V_{BO}	V_{ad}	V_{rel}	V_{QED}	V
3.0	3767.681(71)	1.387(7)	-0.2197(23)	0.0942(2)	3768.94(7)
4.0	292.570(15)	0.1080(32)	0.0324(14)	0.0089(2)	292.719(15)
5.0	-0.4754(65)	-0.0075(13)	0.0240(2)	-0.001 06(4)	-0.460(7)
5.6	-11.0006(2)	-0.0090(5)	0.015 40(4)	-0.001 35(2)	-10.9955(5)
6.0	-9.6819(23)	-0.0072(3)	0.011 43(5)	-0.001 20(4)	-9.6788(23)
7.0	-4.6225(6)	-0.003 33(7)	0.005 77(3)	-0.000 74(3)	-4.6208(6)
12.0	-0.165 92(2)	-0.000 125(1)	0.000 575(2)	-0.000 13(3)	-0.165 60(3)

The computed values of $V(R)$ were fitted to an analytic function

$$\sum_{k=1}^M e^{-a_k R} \sum_{i=I_0}^{I_1} P_{ik} R^i - \sum_{n=N_0}^{N_1} f_n(\zeta R) \frac{C_n}{R^n}$$

$f_{2n}(x)$ - the Tang-Toennies damping function

$$f_{2n}(x) = 1 - e^{-x} \sum_{k=0}^{2n} \frac{x^{-k}}{k!}$$

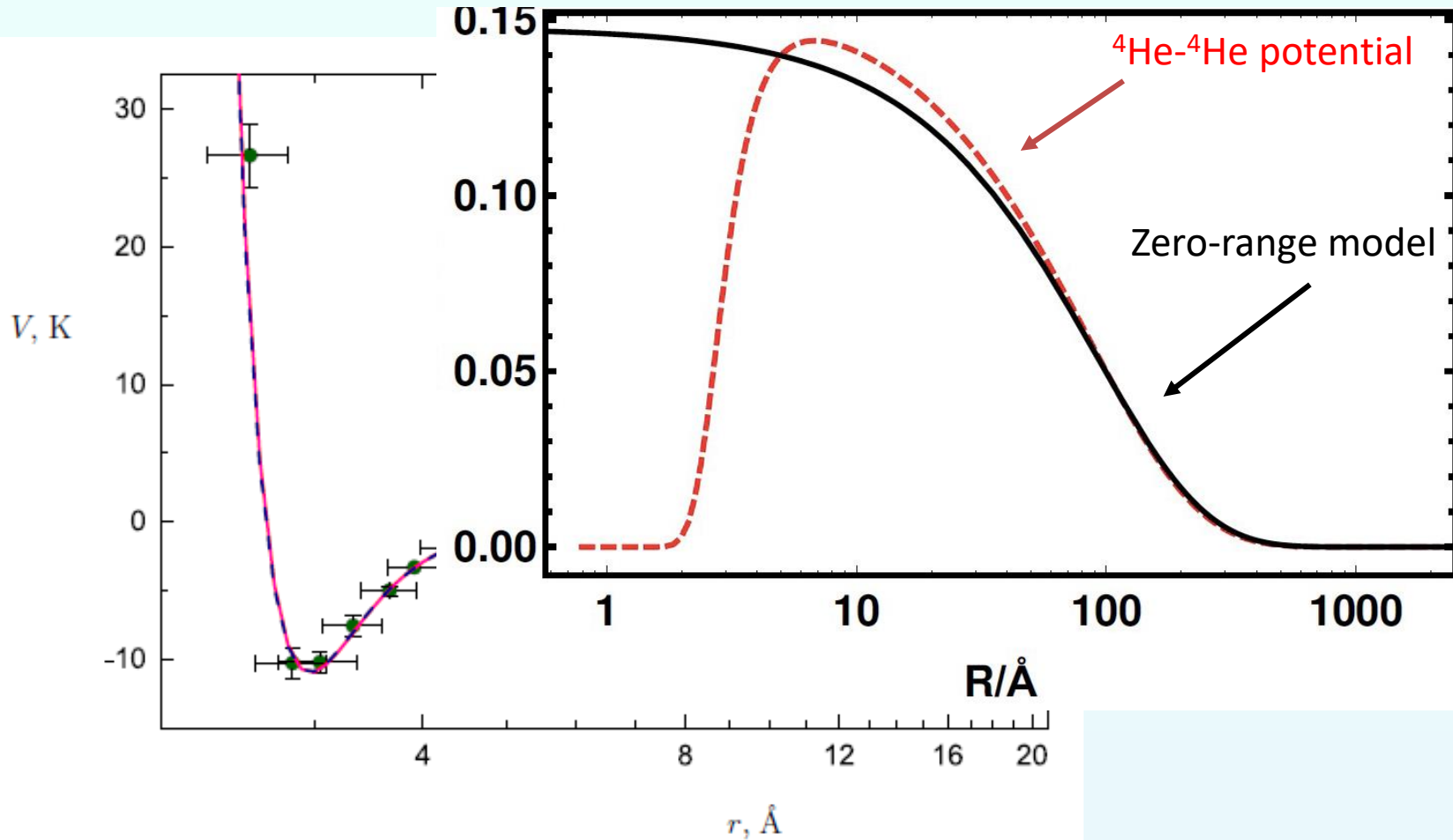
a_k , P_{ik} and ζ are adjustable parameters, and the summation limits $[M, I_0, I_1, N_0, N_1]$

[6] Przybytek M., Cencek W., et. al. // Phys. Rev. Lett. 2010. 104. P. 183003.

[7] Przybytek M., Cencek W., et. al. // Phys. Rev. Lett. 2017. 119. P. 123401.

INTERACTION POTENTIALS

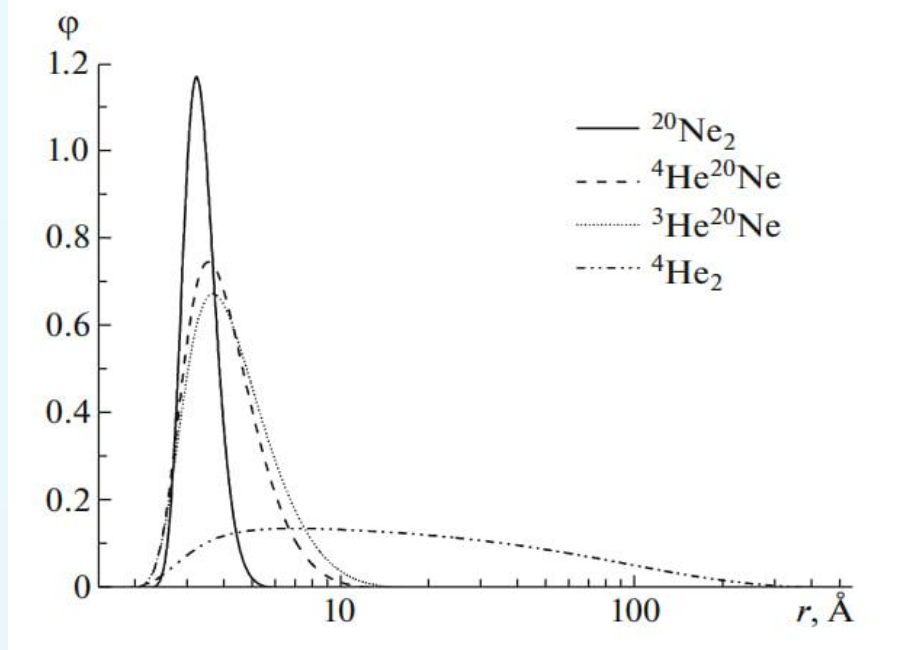
$^4\text{He}_2$

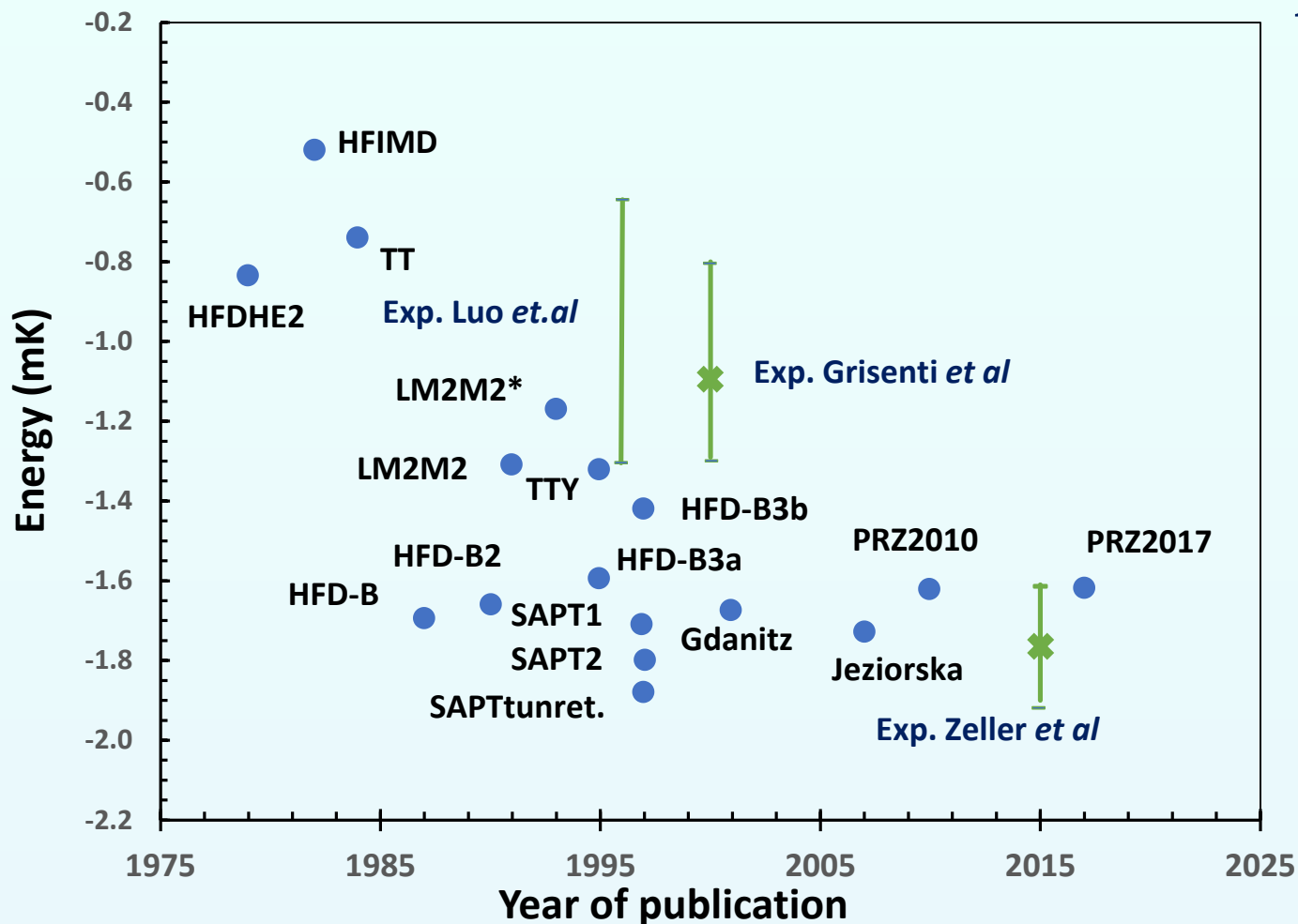


He-He potential $V(r)$, points are experimental data from **S. Zeller et al.**
Phys. Rev. Lett 121 (2018) 083002, blue curve – HFD-B potential (by R.A.Aziz et al.),
red curve – PRZ2010 (by M. Przybytek et al.).

Binding energies	${}^4\text{He}_2$	${}^3\text{He}{}^{20}\text{Ne}$	${}^4\text{He}{}^{20}\text{Ne}$	${}^{20}\text{Ne}_2$
$ E_0 , \text{K}$	0.001316	2.35	3.435	24.1314
$\langle r^2 \rangle^{1/2}, \text{\AA}$	70.6128	4.512	4.140	3.34557
$ E_1 , \text{K}$				4.27744
$\langle r^2 \rangle^{1/2}, \text{\AA}$				4.33144
$ E_2 , \text{K}$				0.0221224
$\langle r^2 \rangle^{1/2}, \text{\AA}$				12.948

Dimers





The predicted values for the helium dimer binding energy using theoretical calculations are displayed alongside experimental measurements

Helium Dimer

$$1 \text{ K} = 8.6 \times 10^{-5} \text{ eV}$$

Using modern Born-Oppenheimer potential:

$$\varepsilon_d = -1.62 \text{ mK} = -5.147 \text{ a.u.}$$

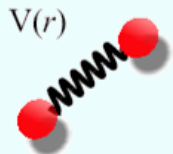
Two-body s-wave scattering length $l_{sc} = 100 \text{ \AA}$

Using zero-range model

$$\varepsilon_d = -\frac{\hbar^2}{ml_{sc}^2} = -4.69 \cdot 10^{-9} \text{ a.u. } (\approx 91\%)$$

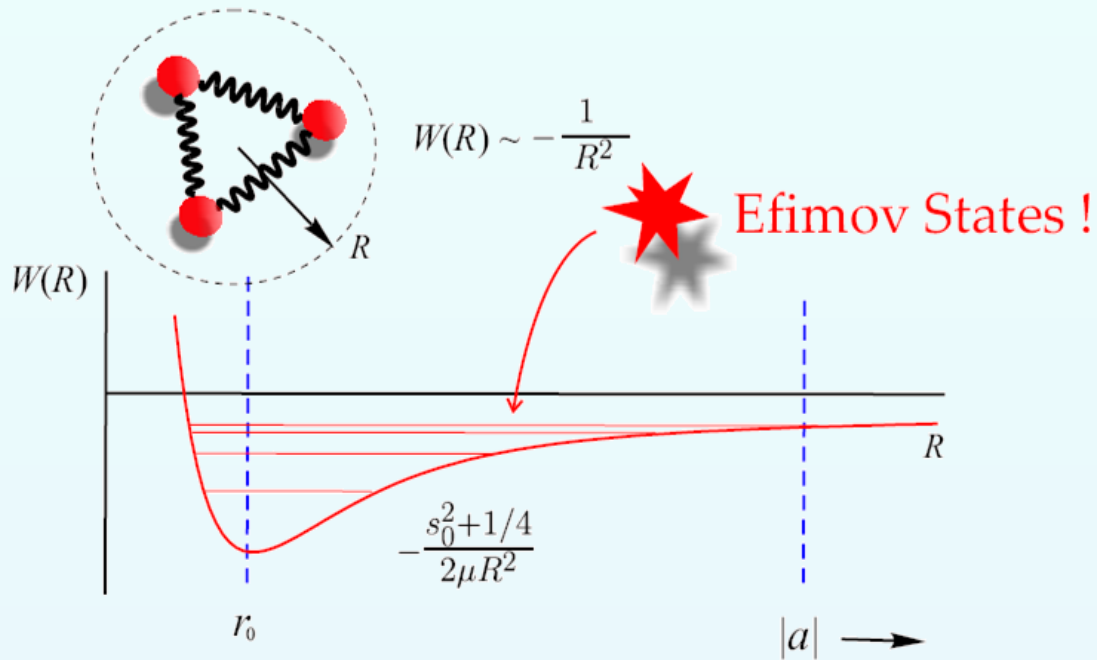
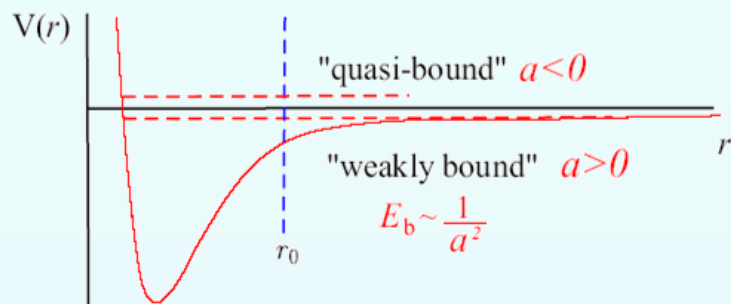
Including effective range correction

$$\varepsilon_d = -\frac{\hbar^2}{mr_{eff}^2} \left(1 - \sqrt{1 - \frac{2r_{eff}}{l_{sc}}}\right)^2 = -5.17 \cdot 10^{-9} \text{ a.u. } (\approx 100\%)$$



Resonant Interaction

$$|a| \gg r_0$$



ENERGY LEVELS ARISING FROM RESONANT TWO-BODY FORCES IN A THREE-BODY SYSTEM

V. EFIMOV

A.F.Ioffe Physico-Technical Institute, Leningrad, USSR

Received 20 October 1970

Resonant two-body forces are shown to give rise to a series of levels in three-particle systems. The number of such levels may be very large. Possibility of the existence of such levels in systems of three α -particles (^{12}C nucleus) and three nucleons (^3H) is discussed.

The range of nucleon-nucleon forces r_0 is known to be considerably smaller than the scattering lengths a . This fact is a consequence of the resonant character of nucleon-nucleon forces. Apart from this, many other forces in nuclear physics are resonant. The aim of this letter is to expose an interesting effect of resonant forces in a three-body system. Namely, for $a \gg r_0$ a series of bound levels appears. In a certain case, the number of levels may become infinite.

Let us explicitly formulate this result in the simplest case. Consider three spinless neutral particles of equal mass, interacting through a potential $gV(r)$. At certain $g = g_0$ two particles get bound in their first s-state. For values of g close to g_0 , the two-particle scattering length a is large, and it is this region of g that we shall confine ourselves to. The three-body continuum boundary is shown in the figure by cross-hatching. The effect we are drawing attention to is the following. As g grows, approaching g_0 , three-par-

ticle bound states emerge one after the other. At $g = g_0$ (infinite scattering length) their number is infinite. As g grows on beyond g_0 , levels leave into continuum one after the other (see fig. 1).

The number of levels is given by the equation

$$N \approx \frac{1}{\pi} \ln(|a|/r_0) \quad (1)$$

All the levels are of the 0^+ kind; corresponding wave functions are symmetric; the energies $E_N \ll 1/r_0^2$ (we use $\hbar = m = 1$); the range of these bound states is much larger than r_0 .

We want to stress that this picture is valid for $a \gg r_0$. Three-body levels appearing at $a \approx r_0$ or with energies $E \approx 1/r_0^2$ are not considered.

The physical cause of the effect is in the emergence of effective attractive long-range forces of radius a in the three-body system. We can demonstrate that they are of the $1/R^2$ kind; $R^2 = r_{12}^2 + r_{23}^2 + r_{31}^2$. This form is valid for $R \gtrsim r_0$. With $a \rightarrow \infty$ the number of levels becomes infinite as in the case of two particles interacting with attractive $1/r^2$ potential.

Thomas and Efimov effects

1. L.H. Thomas (1935)

*Phys. Rev.*47, 903 (1935).

- a) 2-particle potentials are short-range
- b) Each of them supports only a single bound state even with an arbitrarily weak binding energy

Nevertheless, the three-body ground state energy can go to $(-\infty)$ when the range of the two-body forces approaches zero!

(Just this surprising phenomenon is called the Thomas effect.)

I.e., such a three-body system should collapse! \Rightarrow The 3-body Hamiltonian with zero-range interaction is not semibounded from below.

2. V. Efimov (1970)

*Phys. Lett.*33, 563 (1970).

When one weakens the two-body potentials (supporting a single bound state) the number of 3-body bound states can increase to infinity! And this happens at the moment when the two-body bound states disappear.

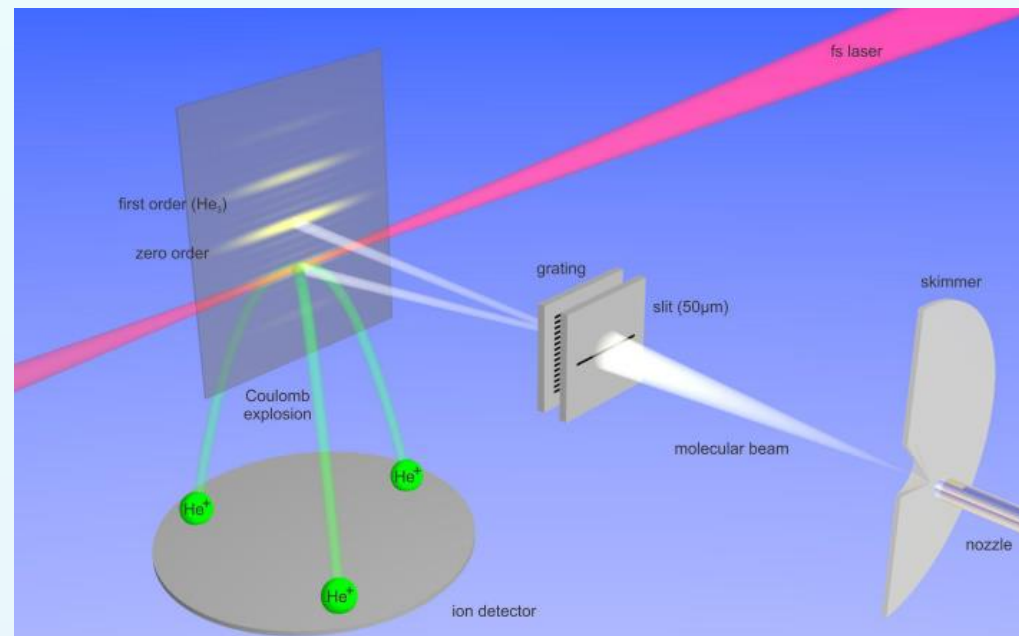
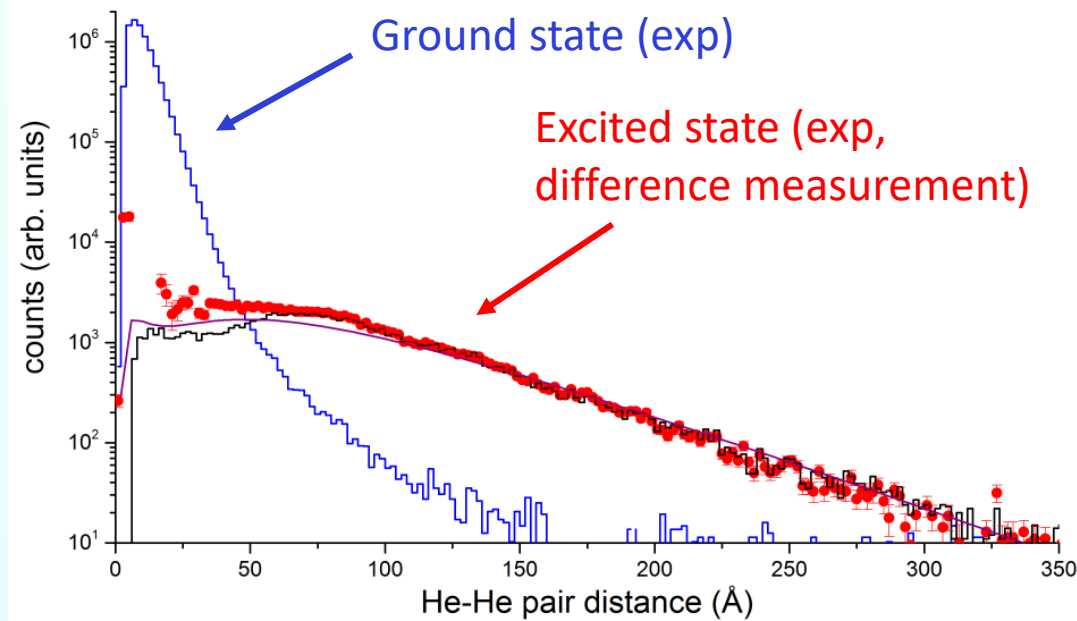
\Rightarrow Efimov states \Leftrightarrow the states which appear under weakening and disappear under strengthening of the two-body potentials.

Experimental observation of the Efimov state of the helium trimer.

Pair distance distributions $P_{\text{pair}}(R)$ of the He_3 excited state. The red circles represent the difference between the mixture of the excited and ground state distribution and the ground state only distribution. The black histogram corresponds to the distribution that was obtained from the measured momenta of the ground and excited state mixture by filtering out the structures with higher KERs. Experimental distributions have been reconstructed from the measured momenta to invert the Coulomb explosion.

$$\epsilon_d - E^* = 0.98 \pm 0.2 \text{ mK}$$

Selection of He trimers from the molecular beam by means of matter wave diffraction.



Helium dimer and trimers

${}^4\text{He}_2$

Bound state energy - $\epsilon_d \approx -1.7 \text{ mK}$

No rotational $J>0$ bound states

${}^3\text{He}$ - ${}^4\text{He}$ does not support bound states

Two-body s-wave scattering length $l_{sc} = 100^{+8}_{-7.9} \text{ \AA}$

Two-body effective range $r_s \approx 7.2 \text{ \AA}$

${}^4\text{He}_3$

Two $J = 0$ bound states - $\approx -131 \text{ mK}$ and -2.6 mK

No rotational $J>0$ bound states

$$1 \text{ K} = 8.6 \times 10^{-5} \text{ eV}$$

Helium dimer and trimers

${}^4\text{He}_2$

Bound state energy - $\varepsilon_d \approx -1.7 \text{ mK}$

No rotational $J>0$ bound states

${}^3\text{He}$ - ${}^4\text{He}$ does not support bound states

Two-body s-wave scattering length $l_{sc} = 100^{+8}_{-7.9} \text{ \AA}$

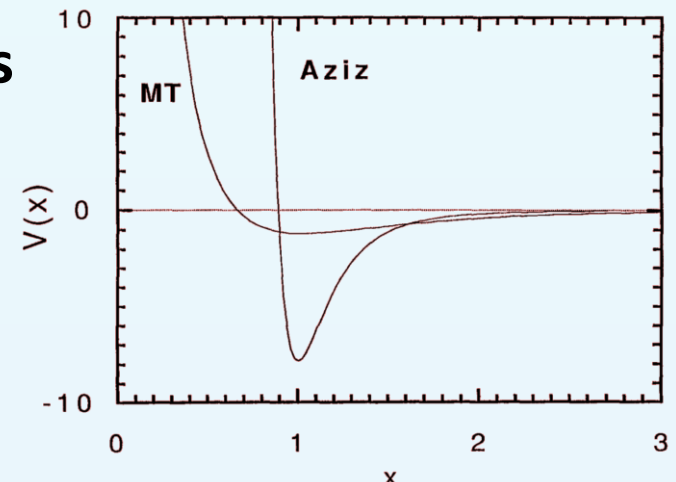
Two-body effective range $r_s \approx 7.2 \text{ \AA}$

${}^4\text{He}_3$

Two $J = 0$ bound states - $\approx -131 \text{ mK}$ and 2.6 mK

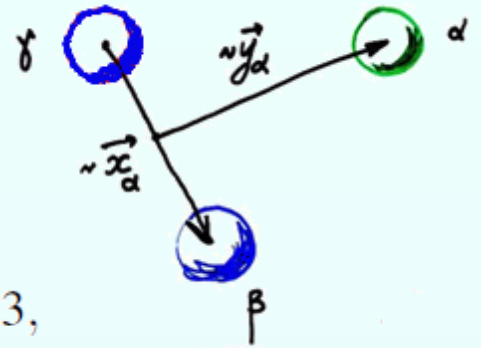
No rotational $J>0$ bound states

Nuclear physics: Deuteron and Triton



${}^3\text{He}{}^4\text{He}_2$ & ${}^4\text{He}_3$

For two ${}^4\text{He}$ atom the corresponding Faddeev component $F_3(\mathbf{x}_3, \mathbf{y}_3)$ is invariant under the permutation of the 1 and 2 particles



$$(-\Delta_X - E)F_\alpha(\mathbf{x}_\alpha, \mathbf{y}_\alpha) = -V_\alpha(\mathbf{x}_\alpha)\Psi^{(\alpha)}(\mathbf{x}_\alpha, \mathbf{y}_\alpha), \quad \alpha = 1, 3,$$

where $\Psi^{(1)}(\mathbf{x}_1, \mathbf{y}_1)$ and $\Psi^{(3)}(\mathbf{x}_3, \mathbf{y}_3)$ denote the total wave function in terms of the Faddeev components

$$\begin{aligned} \Psi^{(1)}(\mathbf{x}_1, \mathbf{y}_1) = & F_1(\mathbf{x}_1, \mathbf{y}_1) \\ & + F_1(c_{21}\mathbf{x}_1 + s_{21}\mathbf{y}_1, -s_{21}\mathbf{x}_1 + c_{21}\mathbf{y}_1) \\ & + F_3(c_{31}\mathbf{x}_1 + s_{31}\mathbf{y}_1, -s_{31}\mathbf{x}_1 + c_{31}\mathbf{y}_1) \end{aligned}$$

$$\begin{aligned} \Psi^{(3)}(\mathbf{x}_3, \mathbf{y}_3) = & F_3(\mathbf{x}_3, \mathbf{y}_3) \\ & + F_1(c_{13}\mathbf{x}_3 + s_{13}\mathbf{y}_3, -s_{13}\mathbf{x}_3 + c_{13}\mathbf{y}_3) \\ & + F_1(c_{23}\mathbf{x}_3 + s_{23}\mathbf{y}_3, -s_{23}\mathbf{x}_3 + c_{23}\mathbf{y}_3). \end{aligned}$$

Expanding Faddeev components in a series of bispherical harmonics we have

$$F_\alpha(\mathbf{x}, \mathbf{y}) = \sum_l \frac{f_l^{(\alpha)}(x, y)}{xy} \mathcal{Y}_{l0}(\hat{x}, \hat{y}), \quad \alpha = 1, 3, \quad x = |\mathbf{x}|, y = |\mathbf{y}|, \hat{x} = \mathbf{x}/x, \text{ and } \hat{y} = \mathbf{y}/y.$$

The energy of the excited state of helium trimer with respect to the two-particle threshold $|E_1 - \varepsilon_d|$, calculated for different potentials and experimental results from [2].

Potential	HFD-B [6]	LM2M2 [14]	TTY [5]	PRZ2010 [3]	PRZ2017 [4]	Exp. [2]
$ E_1 - \varepsilon_d $	1.049	0.972	0,970	0.803	0.802	0.98 ± 0.2

[2] Kunitski M., Zeller S., Voigtsberger J., Kalinin A., Schmidt L.Ph.H., Schoeffler M., Czasch A., Schöllkopf W., Grisenti R.E., Jahnke T., Blume D., Doerner R. // Science. 2015. 348. P. 551.

[3] Przybytek M., Cencek W., Komasa J., Lach G., Jeziorski B., Szalewicz K. // Phys. Rev. Lett. 2010. 104. P. 183003.

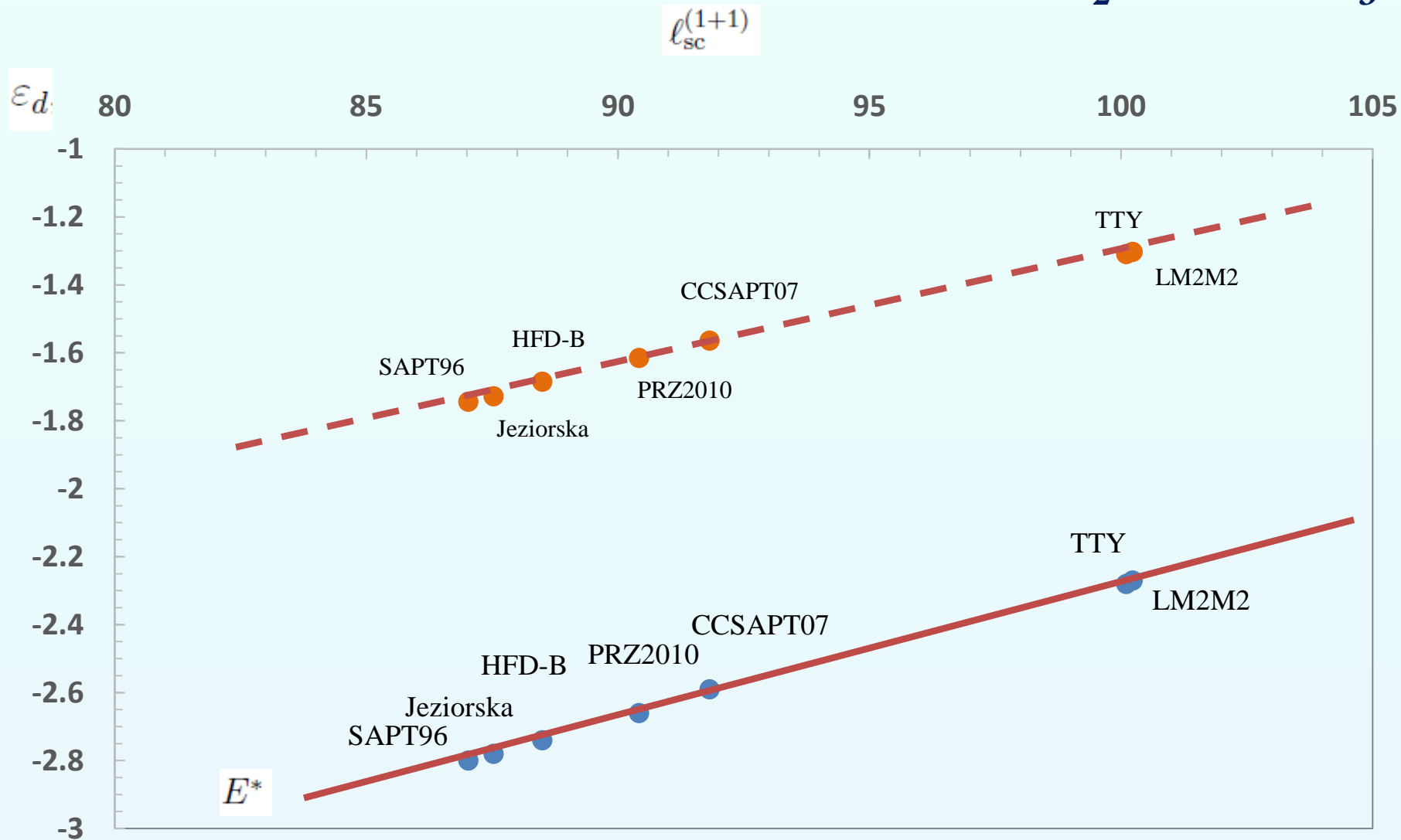
[4] Przybytek M., Cencek W., Jeziorski B., Szalewicz K. // Phys. Rev. Lett. 2017. 119. P. 123401.

[5] Tang K.T., Toennis J.P., Yiu C.L. // Phys. Rev. Lett. 1995. 74. P. 1546

[6] Aziz R.A., McCourt F.R.W., Wong C.C.K. // Mol. Phys. 1987. 61. P. 1487.

[14] Aziz R.A., Slaman M.J. // J. Chem. Phys. 1991. 94. P. 8047-8053.

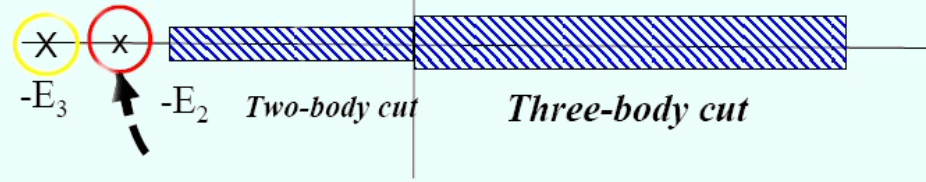
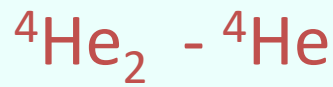
${}^4\text{He}_2$ and ${}^4\text{He}_3$



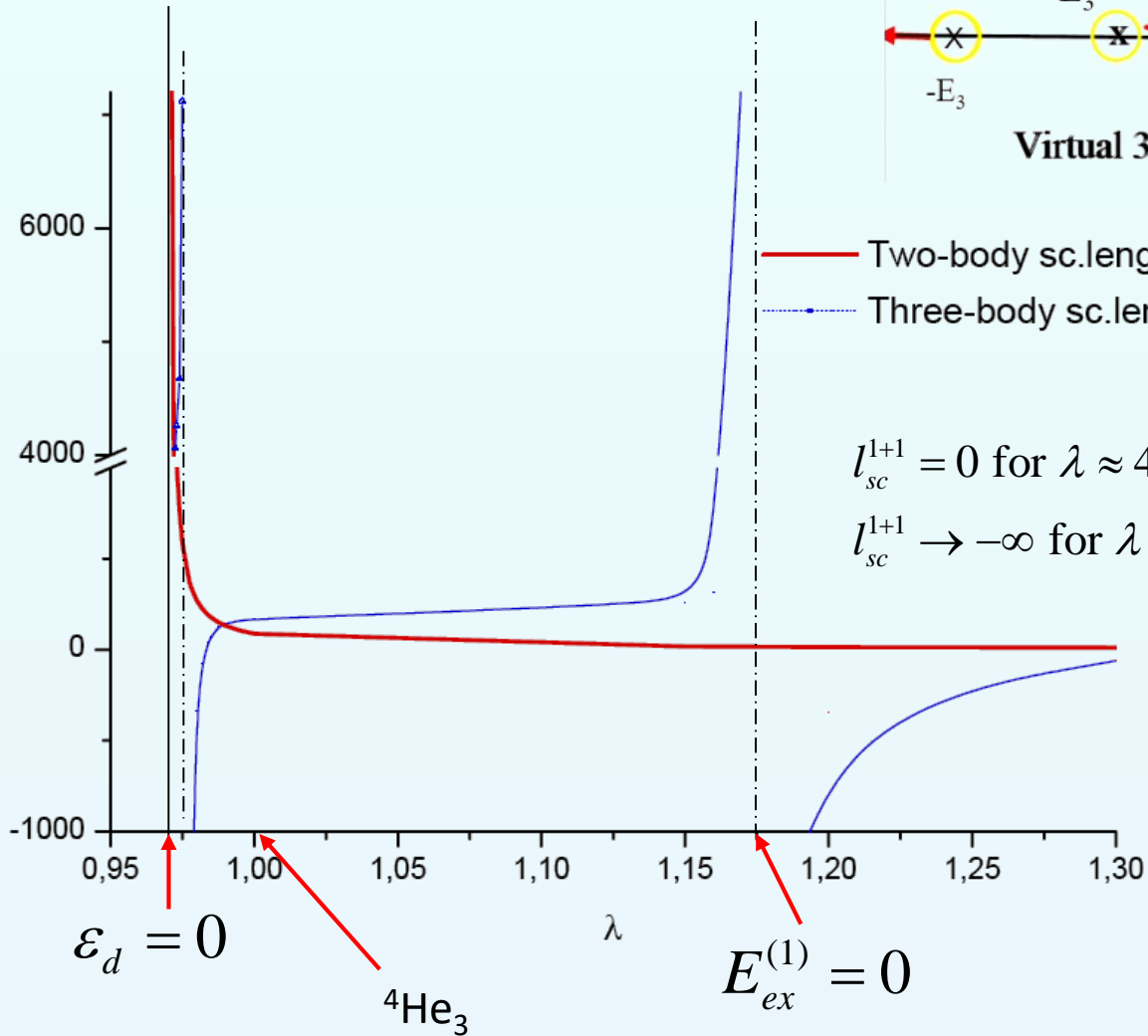
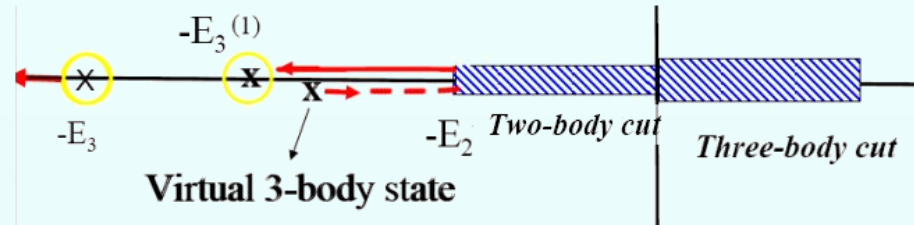
Summary

- Helium small clusters can be realized experimentally and even to study structure. The experimental observation would be more than welcome! Connections to experiments has been and will continue to be very important.
- ^4He - ^4He can be well described by zero-range model, using just two parameters. Simple approaches are helpful to feel things.
- Few-body physics can help to answer fundamental question in an unambiguous, clean, and precise way.
- Still much to understand Efimov physics of weakly bound systems.

Thank you for your attention



$$V(x) = \lambda V_{\text{HFD-B}}(x)$$



— Two-body sc.length $l_{sc}^{(1+1)}$
 - - - Three-body sc.length $l_{sc}^{(2+1)}$

$$l_{sc}^{1+1} = 0 \text{ for } \lambda \approx 4.8$$

$$l_{sc}^{1+1} \rightarrow -\infty \text{ for } \lambda \approx 6.8$$

E.A.Kolganova, A.Motovilov,
Phys. At. Nucl. **62**, 1179 (1999)

M. T. Yamashita, T. Frederico,
 A. Delfino, L. Tomio,
Phys. Rev. A **66**, 052702 (2002)

E.A.Koganova, A.Motovilov,
 W.Sandhas *Nucl.Phys. A* **790**,
 752 (2007)